

## Phase diagram of the Blume-Emery-Griffiths model on the honeycomb lattice calculated by the cluster-variation method

Anders Rosengren and Saulius Lapinskas\*

*Department of Theoretical Physics, Royal Institute of Technology, S-100 44 Stockholm, Sweden*

(Received 27 July 1992)

The cluster-variation method (CVM) is used to study the phase diagram of a spin-1 Ising model with both bilinear and biquadratic nearest-neighbor interactions and with a single-ion potential, on a honeycomb lattice. Since exact results are scarce for this model except for the honeycomb lattice, we argue that approximation schemes should be tested on this lattice. The results for the CVM compare favorably with the exact results. A comparison with other approximate techniques is made. Further, field-induced phase transitions are investigated.

### I. INTRODUCTION

The Blume-Emery-Griffiths (BEG) model is a model with a very rich phase diagram. The model exhibits a wide variety of transitions of first and larger order. We study here the BEG model on a two-dimensional lattice, the honeycomb lattice. It is a spin-1 Ising model with the Hamiltonian

$$\mathcal{H} = -J \sum_{\langle ij \rangle} s_i s_j - K \sum_{\langle ij \rangle} s_i^2 s_j^2 + \Delta \sum_i s_i^2, \quad (1)$$

where  $s_i = 0, \pm 1$ , and  $\langle ij \rangle$  indicates summation over nearest-neighbor points. The model was introduced by Blume, Emery, and Griffiths<sup>1</sup> to describe phase separation and superfluid ordering in He<sup>3</sup>-He<sup>4</sup> mixtures. With  $K = 0$ , the model is known as the Blume-Capel model.<sup>2,3</sup> The model has been reinterpreted to describe phase transitions in simple and multicomponent fluids, metamagnets, and ternary alloys. The model has been extensively studied by means of the mean-field approximation,<sup>1,4-6</sup> by renormalization-group techniques,<sup>7-9</sup> series-expansion methods,<sup>10</sup> and by Monte Carlo methods.<sup>11-14</sup>

Most treatments have been considering the model for  $J + K > 0, J > 0$ . Recently the existence of a new phase was obtained from a Monte Carlo simulation<sup>14</sup> for a planar square lattice with interaction parameters, including the region  $J + K < 0$ . The new ordered phase is a staggered quadrupolar phase with two interpenetrating sublattices. One sublattice has  $s_i = 0$  at every site; the other sublattice has its sites occupied at random by  $s_i = \pm 1$ . Most studies for two-dimensional lattices, like the Monte Carlo study mentioned above, are performed for the square lattice for which very few exact results are available. For the honeycomb lattice, on the contrary, the BEG model was solved *exactly* by graph-theoretical methods of Rosengren and Häggkvist,<sup>15</sup> and other methods by Horiguchi<sup>16</sup> and Wu,<sup>17</sup> for a surface in the three-dimensional space spanned by the coupling constants  $J, K$ , and  $\Delta$ . This exact result provides an excellent tool for comparing the accuracy of the different approximation schemes mentioned above. In this paper we perform a calculation of the phase diagram of the BEG model on the honeycomb lattice by means of the cluster-

variation method and compare this with both the exact<sup>15-17</sup> and approximate results obtained by the graph-theoretical method of Rosengren and Häggkvist<sup>15</sup> outside the surface. In two recent papers, Kaneyoshi<sup>18,19</sup> has obtained the phase diagram for the honeycomb lattice by means of the correlated-effective-field method (CEFT). Gwa and Wu also partly represented the critical phase boundary.<sup>20</sup> The phase diagram obtained by Kaneyoshi is different from ours. We do not find occurrence of reentrant phenomena as he does. Further, the phase diagram at  $T = 0$  suggested by Kaneyoshi is very different from ours. The step-like behavior of the magnetization and quadrupolar moments at a low temperature as a function of applied field found by him is different from our result.

The outline of this paper is as follows: Sec. II describes in short the specific features of the cluster-variation method when applied to the BEG model. In Sec. III our results for the phase diagram of the BEG model in zero magnetic field are noted and a comparison is given with the exact results,<sup>15-17</sup> as well as the approximate results.<sup>15</sup> Some comparison is also made with the results obtained by the correlated-effective-field theory.<sup>18</sup> Also, the similarity with Monte Carlo results<sup>14</sup> obtained for the square lattice is noted. Further, the location of the Potts points<sup>7,21,22</sup> is discussed. In Sec. IV our results for a field-induced phase transition are given. Section V is a summary.

### II. METHOD

The modified version<sup>23</sup> of the cluster-variation method (CVM) with a six-point hexagonal basic cluster was used for the calculation of the phase diagram for the BEG model at finite temperatures. The details of the formulae can be found in the above reference; we here only note features specific to the BEG mode. The cluster Hamiltonian considered is as follows:

$$\begin{aligned} \mathcal{H}_k = & \sum_{\langle ij \rangle} (-J + \psi_k^1) s_i s_j + \sum_{\langle ij \rangle} (-K + \psi_k^2) s_i^2 s_j^2 \\ & + \sum_{\langle ij \rangle} \psi_k^3 (s_i^2 s_j + s_i s_j^2) + \sum_i (\Delta + \varphi_k^1) s_i^2 + \sum_i \varphi_k^2 s_i, \end{aligned} \quad (2)$$

where sums run over all points and nearest-neighbor pairs of the cluster  $k$ . There are two subclusters of the basic ( $k=6$ ) cluster involved in the approximation, namely the two-point cluster ( $k=2$ ) consisting of the two neighboring spins, and a single-point cluster ( $k=1$ ). The free energy per spin of the honeycomb lattice is expressed as

$$F = \frac{1}{2}F_6 - \frac{3}{2}F_2 + F_1, \quad (3)$$

where  $F_k = -k_B T \ln \text{Tr} \exp(-\beta \mathcal{H}_k)$ ,  $\beta = 1/k_B T$ . The effective coupling parameters  $\psi_k^i$  and effective cluster fields  $\varphi_k^i$  ( $\varphi_k^1$  being a quadrupolar field) are found from the self-consistency relations for various statistical moments calculated with the cluster density matrices  $\rho_k = \exp[\beta(F_k - \mathcal{H}_k)]$ . If we by  $\langle \dots \rangle_k$  denote the average with respect to the density matrix of the  $k$  cluster, these relations for the ferromagnetic phase can be written in the following way:

$$\begin{aligned} \langle s_i s_j \rangle_6 &= \langle s_i s_j \rangle_2, \\ \langle s_i^2 s_j^2 \rangle_6 &= \langle s_i^2 s_j^2 \rangle_2, \\ \langle s_i^2 s_j \rangle_6 &= \langle s_i^2 s_j \rangle_2, \\ \langle s_i^2 \rangle_6 &= \langle s_i^2 \rangle_2 = \langle s_i^2 \rangle_1, \\ \langle s_i \rangle_6 &= \langle s_i \rangle_2 = \langle s_i \rangle_1. \end{aligned} \quad (4)$$

The remaining linear relations between  $\psi$ -s and  $\varphi$ -s are obtained from the condition of minimum of  $F$  [Eq. (3)]. For the single-sublattice (ferromagnetic) phase these are

$$\begin{aligned} 2\psi_6^i - \psi_2^i &= 0, \quad i = 1, 2, 3, \\ 3(\varphi_6^i - \varphi_2^i) + \varphi_1^i &= 0, \quad i = 1, 2. \end{aligned} \quad (5)$$

The relations (5) actually reduce the number of linearly independent variational parameters  $\psi$  and  $\varphi$ . For the single-sublattice phase we have 7 independent parameters, while for the two-sublattice phase the number of parameters increases to 12. We should also notice that two different single-point clusters are introduced in the latter case, one for each sublattice.

Thus, to obtain the equilibrium values of the variation parameters we solve the set of nonlinear equations (4) using the usual Newtonian method. The phase transitions are detected in a traditional way. The second-order transition is recognized from the splitting of one degenerate free-energy minimum into two. The first-order transition corresponds to the shift of the global minimum between two local minima  $\langle s_i \rangle$ ,  $\langle s_i^2 \rangle$ ,  $\langle s_i s_j \rangle$ , etc.). There may exist several solutions of the equations (4) with different  $F$ 's and we choose the lowest one.

### III. RESULTS

The ground-state analysis of the BEG model on the honeycomb lattice can be confined to single- and two-sublattice structures since the interaction is limited to nearest neighbors only. For  $J > 0$ , one could expect two single sublattice phases: a paramagnetic ( $P$ ) with all spins  $s_i = 0$  and a double-degenerate ferromagnetic ( $F$ )

with all  $s_i = +1$  or  $-1$ . At large negative  $K$ , a two-sublattice staggered quadrupolar (SQ) phase is expected with all  $s_i = 0$  for one sublattice and randomly distributed nonzero spins for another. Such a phase was actually observed in Monte Carlo simulations on the square and simple cubic lattices.<sup>13,14</sup> This phase is a highly degenerate "frustrated" structure with the finite entropy  $s = \ln 2/2$  per spin at  $T = 0$ .

The lines separating these three phases at  $T = 0$  can be obtained by comparing the ground-state energies of the phases. These are as follows:

$$\begin{aligned} E_P &= 0, \\ E_F &= -\frac{3}{2}(J + K) + \Delta, \\ E_{SQ} &= \Delta/2. \end{aligned} \quad (6)$$

The equations  $E_P = E_F$ ,  $E_P = E_{SQ}$ ,  $E_F = E_{SQ}$  yield the straight lines separating the phases  $P$ - $F$ ,  $P$ - $SQ$ , and  $F$ - $SQ$ , respectively, which in the space  $k = K/J$ ,  $d = \Delta/J$  can be written as

$$\begin{aligned} d &= \frac{3}{2}(k + 1), \\ d &= 0, \\ d &= 3(k + 1). \end{aligned} \quad (7)$$

All three phases meet in the point ( $k = -1$ ,  $d = 0$ ).

The BEG phase diagram as obtained in the CVM treatment is presented in Fig. 1 in the  $(T/J, K/J)$  plane. The solid lines represent the second-order phase-transition boundaries and the dotted lines the first-order phase-transition boundaries. The boundaries are labeled with the crystal-field interaction parameter  $\Delta$  in units of  $J$ . The dashed line represents the surface  $K/k_B T = -\ln \cosh(J/k_B T)$  on which the BEG model is exactly solved. The dash-dotted lines are the second-order phase-transition boundaries obtained by the approximate treatment.<sup>15</sup> In that treatment another model was exactly solved, which, on the surface  $K/k_B T = -\ln \cosh(J/k_B T)$  coincided with the BEG model. The points of intersection of the dash-dotted lines and the dashed line are therefore exact for the BEG model. Let us first consider the curve  $d = \Delta/J = 0$ . It is a second-order phase-transition boundary, separating the ferromagnetic and the paramagnetic phase. Except for the two points of intersection between the dash-dotted curve  $d = 0$  and the dashed curve which are exact, there are two more points where a comparison could be made. At  $k = 0$ , the BEG model is reduced to the spin-1 Ising model. The low-temperature series expansions by Fox and Guttman<sup>24</sup> give  $k_B T_c/J = 1.158\dots$  for this model. Further for  $K \rightarrow \infty$ , the BEG model is equivalent to the spin-1/2 Ising model and therefore  $\tanh(J/k_B T_c) = 1/\sqrt{3}$ , i.e.,  $k_B T_c/J = 1.5186\dots$ . The approximate treatment by Rosengren and Häggkvist<sup>15</sup> is therefore correct in the three above-mentioned points and close to the fourth point. The solid line ( $d = 0$ ), which is the CVM result, is slightly above the dash-dotted line ( $d = 0$ ) for all  $K/J > -1$  and has, of course, the wrong limit for  $K \rightarrow \infty$ . So for  $d = 0$  the approximate treatment in Ref.

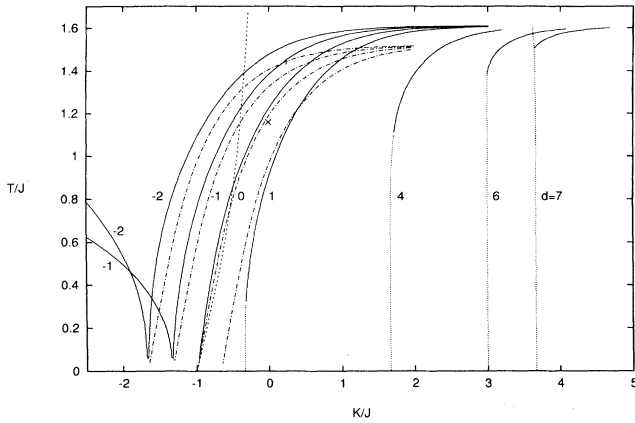


FIG. 1. Calculated phase diagram of the BEG model. The solid and dotted lines represent the second- and first-order phase-transition lines, respectively, obtained by the CVM. The dashed-dotted lines are the second-order phase transitions from the approximation of Ref. 15. The dashed line is the surface on which the treatment (Ref. 15) is exact. The lines are labeled with the values of  $d = \Delta/J$ . The cross denotes the estimate (Ref. 22) of  $T_c/J$  for  $K = \Delta = 0$ .

15 is better. The corresponding results from the CEFT model are much above the CVM result. For  $d < 0$ , a new ordered phase occurs in the CVM results in the region  $K/J < -1$ , with two interpenetrating sublattices; one sublattice has  $s_i = 0$  at every site and the other has sites with  $s_i = \pm 1$ . Such a behavior was also obtained in the MC calculation<sup>14</sup> for the square-lattice phase diagram. The approximate treatment of Ref. 15 cannot be due to the very nature of the approximation, or say anything about such a phase. The  $F$  and  $SQ$  phases meet at  $T = 0$  and at  $K/J = \Delta/3J - 1$ . However, at finite  $T$ , they are everywhere separated by the disordered  $P$  phase. It is worth noticing that such a behavior seems to be common for models exhibiting the frustrated phases with finite  $s(T = 0)$ . For example, the exactly solvable Union Jack

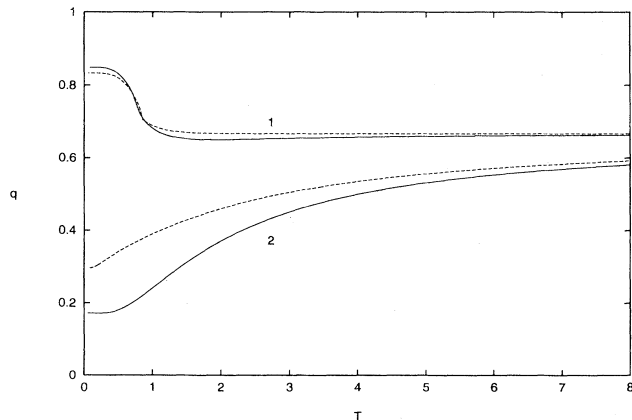


FIG. 2. The temperature dependence of the quadrupolar moment  $q = \langle s_i^2 \rangle$  calculated by the graph theory (Ref. 15) (solid line) and the CVM (dashed line) along the path: (1)  $K/kT = -\ln \cosh(J/kT)$ , (2)  $K = -J$ .  $\Delta = 0$  for all lines.

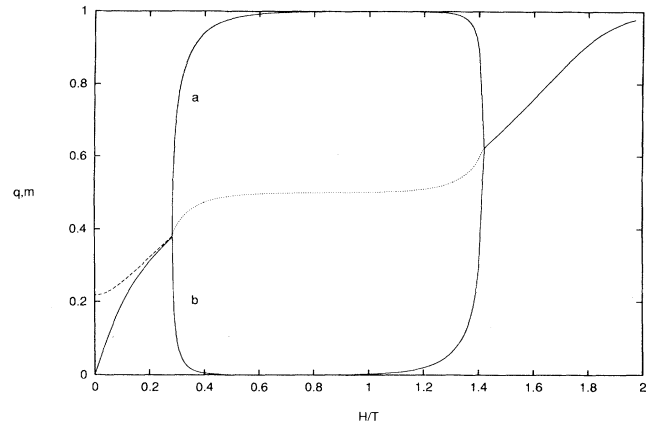


FIG. 3. The field dependence of the magnetization  $m = \langle s_i \rangle$  (solid line) and quadrupolar moment  $q = \langle s_i^2 \rangle$  (dashed line) for the two sublattices  $a$  and  $b$ . The dotted line is  $q$  averaged over both sublattices. The parameters are  $T/J = 0.1$ ,  $K/J = -1.5$ ,  $\Delta/J = 0.1$ .

model<sup>25</sup> (a spin-1/2 model with half of next-nearest-neighbor interactions included) with a frustrated antiferromagnetic phase also shows the ferromagnetic and antiferromagnetic phases separated at finite temperature by the narrow inclusion of the paramagnetic phase. The exact solution also predicts the reentrant phenomena for the antiferromagnetic phase. While no reentrant phenomena were observed in our calculations for the BEG model on the honeycomb lattice, the Monte Carlo calculations yield such a phenomenon for the three-dimensional simple cubic lattice<sup>13</sup> and, probably, also for the two-dimensional square lattice;<sup>14</sup> however, in this case, the  $F$  phase is reentrant. It should be noted that the mean-field treatment gives the reentrant phenomena irrespective of the dimensionality and the coordination number.<sup>26</sup>

For  $d > 0$ , a second-order phase-transition line joins with a first-order phase-transition line at the tricritical point as seen in the CVM treatment. Likewise for this case ( $d > 0$ ) the approximate treatment of Ref. 15 cannot say anything about such behavior. For  $d > 0$  [note that the sign convention used by Kaneyoshi is different from the one used in Eq. (1)], first-order segments of the ferromagnetic phase boundary line show bulges in the CEFT calculation,<sup>18</sup> suggesting the occurrence of reentrant phenomena. No such behavior is found in our results.

The full BEG model Hamiltonian with both even and odd interactions

$$\mathcal{H} = -J \sum_{\langle ij \rangle} s_i s_j - K \sum_{\langle ij \rangle} s_i^2 s_j^2 + L \sum_{\langle ij \rangle} (s_i s_j^2 + s_i^2 s_j) + \Delta \sum_i s_i^2 + H \sum_i s_i \quad (8)$$

obeys the three-state permutation symmetry which follows from a relabeling of spin state which permutes  $s_i = 0, \pm 1$ .<sup>7</sup> From the interchange  $0 \leftrightarrow 1$ , it follows<sup>7</sup> that

$$Z(J, K, \Delta, H, L) = Z(\bar{J}, \bar{K}, \bar{\Delta}, \bar{H}, \bar{L}),$$

for

$$\begin{aligned}\tilde{J} &= \frac{1}{4}(J + K - 2L), \\ \tilde{K} &= \frac{1}{4}(9J + K + 6L), \\ \tilde{\Delta} &= \frac{1}{2}(3zJ + zK - \Delta + 3H + 4zL), \\ \tilde{H} &= \frac{1}{2}(zJ - zK + \Delta + H), \\ \tilde{L} &= \frac{1}{4}(-3J + K + 2L).\end{aligned}\quad (9)$$

Here  $x$  is the coordination number of the lattice. On the line  $K=3J$ ,  $\Delta=2zJ$ ,  $H=L=0$ , each point is mapped onto itself. Further, for this line the BEG Hamiltonian reduces to

$$\mathcal{H} = -R \sum_{\langle ij \rangle} (\delta_{s_i s_j} - 1), \quad (10)$$

where  $R=2J$ . This is the three-state Potts model.<sup>21,22</sup> The three-state Potts transition occurs at  $R/k_B T_p = 2[\cos(2\pi/9) + \cos(\pi/9)] + 1$ , i.e.,  $k_B T_p/J \simeq 1.3475$ . Our CVM calculation gives  $k_B T_p/J \simeq 1.3835$  ( $K/J=3$ ,  $\Delta/J=6$ ) (Fig. 1). Thus also for this point, where a comparison with an exact result could be made, the accuracy of the cluster-variation method proved to be good.

Another special point in the phase diagram of the BEG model is that with  $K/J=-1$ ,  $\Delta/J=0$ ,  $T=0$ . It is at this point where the ground-state phases  $P$ ,  $F$ , and SQ meet. The exact solution<sup>15</sup> on the path  $K/k_B T = -\ln \cosh(J/k_B T)$ ,  $\Delta=0$  reveals that the quadrupolar moment  $q$  tends to the value  $q_0=0.8485$  when approaching that point (Fig. 2). The CVM result on the same path appears to be rather near the exact one, i.e.,  $q_0=0.8323$ . The major difference appears at the  $F \rightarrow P$  phase transition, where CVM yields a kink, while exact calculation shows an inflection point. Nevertheless, quantitatively, both lines are very close to each other.

A fact to notice is that the limiting value  $q_0$  is different when the point  $K/J=-1$ ,  $\Delta/J=0$ ,  $T=0$ , is approached by another path, say the vertical line  $K/J=-1$ ,  $\Delta/J=0$ . In that case the CVM gives  $q_0=0.2959$  and the approximate treatment in Ref. 15 gives  $q_0=0.1716$ . The difference between the two results is much bigger than in the previous case. However, one should remember that the solution<sup>15</sup> is not for the BEG model itself outside the surface  $K/k_B T = -\ln \cosh(J/k_B T)$  and, though at the point  $K/J=-1$ ,  $\Delta/J=0$ ,  $T=0$ , it is exact for the BEG, the limiting value  $q_0$  can be different from the exact value if the path does not lie in the above-mentioned surface. The exact value for  $q_0$  along a vertical line is expected to be close to the CVM value. Kaneyoshi's result on this path is  $q_0 \simeq 0.44$ , which is far above the CVM result. In the limit of infinite temperature, corresponding to the system of noninteracting spins, the limiting value is  $q=2/3$ , irrespective of method and path.

#### IV. FIELD-INDUCED PHASE TRANSITIONS

The external magnetic field  $H$  removes the "frustration" of the ground state of the SQ phase which then

remains double degenerate with  $s(T=0)=0$ . The field is also going to shift the ground-state phase diagram towards positive  $\Delta$ . For small positive  $d$  and  $k < -1$ , this shift gives rise to field-induced phase-transition phenomena. These phenomena were recently investigated by Kaneyoshi.<sup>19</sup> However, his correlated effective-field theory (CEFT) does not consider the two-sublattice phase.

Our CVM calculations of the external field effect on the BEG model for  $k=-1.5$ ,  $d=0.1$  are presented in Fig. 3. They reveal the field-induced SQ phase, which is separated by second-order phase transitions from the low- $q$  ( $q < 0.5$ ) and high- $q$  ( $q > 0.5$ ) single-sublattice phases. The latter two phases correspond to para- and ferromagnetic phases at zero  $H$ . The magnetization  $m$  is nearly saturated ( $m \simeq q$ ) for both the SQ and high- $q$  phases at  $T=0.1$ . No steps at  $q=1/3$  and  $q=2/3$ <sup>19</sup> were observed.

It should be noted that the SQ and high- $q$  phases are no longer separated by an intermediate phase as were the SQ and  $F$  phases at zero field. Actually there is no difference between the  $P$  and  $F$  phases in the field since both have  $m > 0$ . Consequently, there is no para-ferro phase transition. According to the ground-state analysis, both critical fields approach their limiting values  $H_1=\Delta$ ,  $H_2=\Delta-3(1+K)$  with decreasing temperature, while the  $q$  values of the low- $q$  and high- $q$  phases tend to  $q=0$  and  $q=1$  respectively. At  $T=0$ , the applied field switches the spins of one sublattice from 0 to 1 at  $H=H_1$  and spins of the other sublattice are switched to 1 at  $H=H_2$ . So the only plateau on the  $q(H)$  dependence is expected at  $q=1/2$ , corresponding to the average of  $q$ 's over the two sublattices of the SQ phase.

#### V. SUMMARY

The BEG model has been widely studied by many different approximation techniques. For two-dimensional lattices such studies were mostly conducted for the square lattice. However, since the model has been solved exactly for the honeycomb lattice on a surface in the three-dimensional space spanned by its coupling constants, we have argued here that this lattice is a good testing ground for the different approximation schemes. We have calculated the phase diagram of the model on this lattice by the cluster-variation method, and have made a comparison to the exact results known (including the Potts point) and also have made a comparison with other recent approximate treatments undertaken for this model. We find that the cluster-variation method gives a very good overall agreement with what is exactly known. Further, we have investigated the model in an applied magnetic field, and find field-induced phenomena.

#### ACKNOWLEDGMENTS

This work was supported by the Swedish Natural Science Research Council. S. L. thanks the Department of Material Science, the Royal Institute of Technology, Stockholm, and the Swedish Institute for financial support.

- \*Permanent address: Department of Physics, Vilnius University, Sauletekio al. 9, 2054 Vilnius, Lithuania.
- <sup>1</sup>M. Blume, V. J. Emery, and R. B. Griffiths, *Phys. Rev. A* **4**, 1071 (1971).
- <sup>2</sup>M. Blume, *Phys. Rev.* **141**, 517 (1966).
- <sup>3</sup>H. W. Capel, *Physica (Utrecht)*, **32**, 966 (1966); **33**, 295 (1967); **37**, 423 (1967).
- <sup>4</sup>D. Furman, S. Dattagupta, and R. B. Griffiths, *Phys. Rev. B* **15**, 441 (1977).
- <sup>5</sup>J. Lajzerowicz and J. Sivardière, *Phys. Rev. A* **11**, 2079 (1975); J. Sivardière and J. Lajzerowicz, *ibid.* **11**, 2090 (1975); **11**, 2101 (1975).
- <sup>6</sup>D. Mukamel and M. Blume, *Phys. Rev. A* **10**, 619 (1974).
- <sup>7</sup>A. N. Berker and M. Wortis, *Phys. Rev. B* **14**, 4946 (1976).
- <sup>8</sup>M. Kaufman, R. B. Griffiths, J. M. Yeomans, and M. E. Fisher, *Phys. Rev. B* **23**, 3448 (1981).
- <sup>9</sup>Th. W. Burkhardt, *Phys. Rev. B* **14**, 1196 (1976).
- <sup>10</sup>D. M. Saul, M. Wortis, and D. Stauffer, *Phys. Rev. B* **9**, 4964 (1974).
- <sup>11</sup>B. L. Arora and D. P. Landau, in *Magnetism and Magnetic Materials*, Proceedings of the 18th Annual Conference, Denver, CO, 1972, edited by C. D. Graham and J. L. Rhyne, AIP. Conf. Proc. No. 10 (AIP, New York, 1973).
- <sup>12</sup>M. Tanaka and T. Kawabe, *J. Phys. Soc. Jpn.* **54**, 2194 (1985).
- <sup>13</sup>Y. L. Wang and C. Wentworth, *J. Appl. Phys.* **61**, 4411 (1987).
- <sup>14</sup>Y. L. Wang, F. Lee, and J. D. Kimel, *Phys. Rev. B* **36**, 8945 (1987).
- <sup>15</sup>A. Rosengren and R. Häggkvist, *Phys. Rev. Lett.* **63**, 660 (1989).
- <sup>16</sup>T. Horiguchi, *Phys. Lett.* **113A**, 425 (1986).
- <sup>17</sup>F. Y. Wu, *Phys. Lett.* **116A**, 245 (1986).
- <sup>18</sup>T. Kaneyoshi, *Physica A* **164**, 730 (1990).
- <sup>19</sup>T. Kaneyoshi, *J. Magn. Magn. Mater.* **95**, 157 (1991).
- <sup>20</sup>L. H. Gwa and F. Y. Wu, *Phys. Rev. B* **43**, 13 755 (1991).
- <sup>21</sup>R. B. Potts, *Proc. Cambridge Philos. Soc.* **48**, 106 (1952).
- <sup>22</sup>R. J. Baxter, *Exactly Solved Models in Statistical Mechanics* (Academic, London, 1982).
- <sup>23</sup>V. E. Zubkus and S. Lapinskas, *J. Phys. Condens. Mater.* **2**, 1753 (1990).
- <sup>24</sup>P. F. Fox and A. J. Guttmann, *J. Phys. C* **6**, 913 (1973).
- <sup>25</sup>V. G. Vaks, A. I. Larkin, and Yu. N. Ovchinnikov, *Zh. Eksp. Teor. Fiz.* **49**, 1180 (1965) [*Sov. Phys. JETP* **22**, 820 (1966)].
- <sup>26</sup>W. Hoston and A. N. Berker, *Phys. Rev. Lett.* **67**, 1027 (1991).